ARTICLE

Spin-orbit Splitting and Lifetime Broadening in the $A^2\Delta$ Electronic State of l-C_5H

Mohammad Ali Haddad[a], Dong-feng Zhao[a*], Harold Linnartz[a,b], Wim Ubachs[a]

a. Institute for Lasers, Life, and Biophotonics, VU University Amsterdam, De Boelelaan 1081, NL 1081HV Amsterdam, the Netherlands
b. Sackler Laboratory for Astrophysics, Leiden Observatory, University of Leiden, PO Box 9513, NL 2300 RA Leiden, the Netherlands

(Dated: Received on July 22, 2011; Accepted on February 12, 2012)

Optical absorption bands at ∼18772 and ∼18807 cm^{-1}, previously assigned to $A^2\Delta$-$X^2\Pi$ electronic origin band transitions of the linear carbon-chain radicals C_5H and C_5D, respectively, have been reinvestigated. The spectra have been recorded in direct absorption applying cavity ring-down spectroscopy to a supersonically expanding acetylene/helium plasma. The improved spectra allow deducing a l-C_5H upper state spin-orbit coupling constant A'=−0.7(3) cm^{-1} and a $A^2\Delta$ lifetime of (1.6±0.3) ps.

Key words: Cavity ring down spectroscopy, Carbon-chain radical, Interstellar molecule, C_5H

I. INTRODUCTION

Highly unsaturated carbon-chain radicals of the form C_nH have been identified in dark interstellar clouds through comparison of radio-astronomical observations with spectra obtained from microwave laboratory experiments [1, 2]. Among these species, the linear carbon chain radical l-C_5H has been observed around the carbon-rich star IRC+10216 and towards TMC-1 [3, 4]. A linear geometry has been calculated as its most stable isomer [5], and the ground state has been predicted to be a regular $^2\Pi$ state [6]. Dedicated laboratory work on microwave spectra has resulted in a set of accurate ground state parameters for both C_5H and C_5D [7, 8]. Electronic transition band systems of C_5H and C_5D have been reported in a mass-selective REMPI-TOF study in which spectral features at ∼18791 and 18824 cm^{-1} were assigned as origin band transitions from the electronic ground state to an electronically excited $^2\Delta$ state, respectively. This assignment was backed-up by *ab initio* predictions [9]. An $11\sigma\rightarrow3\pi$ electron excitation from a $X^2\Pi$ ground state can result in excited $^2\Sigma^+$, $^2\Sigma^-$, and $^2\Delta$ states, and theoretical work shows that for C_5H the $^2\Delta$ state is the lowest among these states [10].

In this study, improved spectra are presented for the $A^2\Delta$-$X^2\Pi$ electronic origin band transitions of l-C_5H and l-C_5D, using a different technique based on cavity ring-down spectroscopy. The wavelength calibration is improved compared to previous work [9]. The spin-orbit splitting in the upper electronic $^2\Delta$ state of l-C_5H is determined. A contour analysis of the unresolved band profiles allows an estimate for the $A^2\Delta$ state lifetime.

II. EXPERIMENTS

Pulsed cavity ring-down (CRD) spectroscopy is used to record direct absorption spectra of C_5H and C_5D through a supersonically expanding hydrocarbon plasma. The expansion crosses the central axis of a high finesse optical cavity. This cavity consists of two highly reflective planoconcave mirrors (Research Electro-Optics, reflectivity ∼99.998% at 532 nm) positioned 58 cm apart and mounted on high precision alignment tools that are located on opposite sites of a high vacuum chamber. The latter is evacuated by a roots blower system with 1200 m^3/h pumping capacity. Tunable light in the 532 nm region is obtained from a Nd:YAG (355 nm) pumped dye laser (Sirah, Cobra-Stretch) that is focused into the cavity and light leaking out of the cavity is detected by a photo-multiplier visualizing separate ring-down events. Typical ring down events are of the order of 60 μs. The dye laser has a bandwidth of ∼0.07 cm^{-1} and this can be further improved to ∼0.035 cm^{-1} using the second order diffraction of the Littrow grating in the oscillator [11, 12]. An absolute frequency calibration is achieved with a precision better than 0.02 cm^{-1} by simultaneously recording an I_2 reference spectrum. The system runs at 10 Hz and an accurate triggering scheme is used to temporally overlap the plasma pulse and the ringdown event.

Two different plasma sources are used. The design and operation of a pinhole plasma source has been documented in Ref.[13]. As a precursor gas for C_5H (or

*Author to whom correspondence should be addressed. E-mail: d.zhao@vu.nl

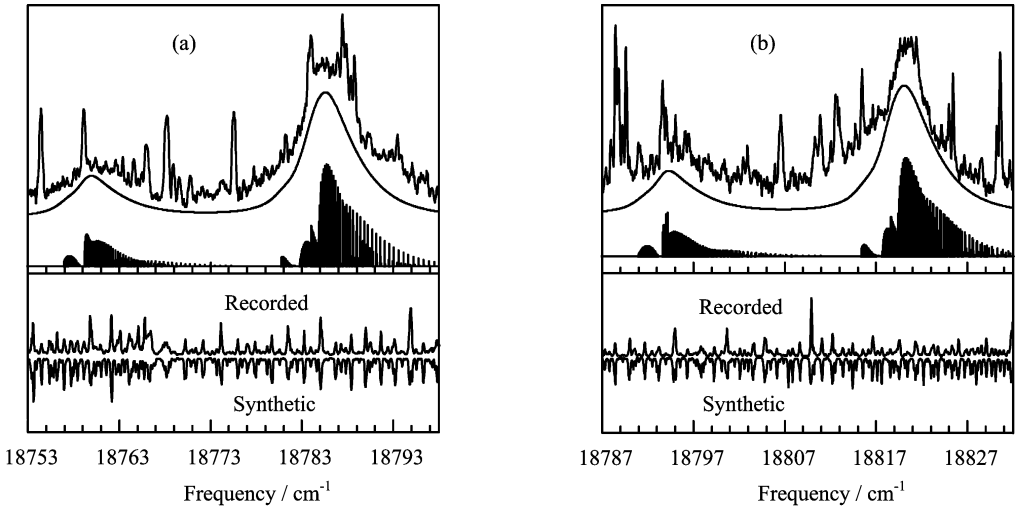

FIG. 1 $A^2\Delta$-$X^2\Pi$ origin band spectra for (a) C_5H and (b) C_5D. The upper traces in both panels show the cavity ring-down recordings using a pinhole nozzle. The sharp features in the observed spectra are due to overlapping absorptions of small radicals. The middle traces are the simulated spectra for a Lorentzian line width of Γ=3.3 cm^{-1} and a Gaussian line width of 0.12 cm^{-1} assuming a rotational temperature of 30 K. The stick diagrams are simulations for a $A^2\Delta$-$X^2\Pi$ transition using the molecular parameters listed in Table I. The simultaneously recorded I_2 reference spectra are also shown in the lower traces of both panels and matched to the synthetic I_2 spectrum for absolute frequency calibration.

C_5D) a mixture of 0.4%C_2H_2/He (or 0.3%C_2D_2/He) is expanded with a backing pressure of ∼0.7 MPa through an orifice (ϕ≈1.2 mm). The gas mixture is discharged by applying a ∼300 μs long high voltage pulse (−1 kV/100 mA) during of ∼1 ms. Typical pressure in the vacuum chamber amounts to ∼1 Pa during plasma operation. The best achievable spectral resolution is limited to ∼0.12 cm^{-1} because of residual Doppler broadening in the pinhole jet expansion. The distance of the pinhole nozzle orifice to the optical cavity axis is set to 2 mm for C_5H (and C_5D) spectra recording, yielding an approximate rotational temperature of T_{rot}≈30 K.

An improvement in spectral resolution is possible, using a 3 cm×200 μm slit discharge nozzle. This system has been used in many studies and details are available from Ref.[14]. The resulting planar plasma provides a nearly "Doppler-free" environment and the linewidth is expected to be limited by the laser bandwidth. In addition, the effective absorption path length is longer. A diluted gas mixture of 1%C_2H_2/He is used and discharged at ∼1 MPa backing pressure by applying a ∼400 μs long high voltage pulse (−750 V/100 mA) during a ∼1 ms gas pulse. In this case the typical pressure in the chamber is ∼4 Pa during slit jet operation. As the gas consumption in the slit nozzle geometry is substantial, only experiments for C_2H_2/He plasma expansions are performed.

The experiment is not mass selective and different transient molecules are formed simultaneously in the plasma jet. Consequently, besides the C_5H/C_5D spectra additional and (partially) overlapping transitions from other species are recorded. An unambiguous identification, however, is possible following the data recorded in the mass-selective REMPI-TOF experiment [9].

III. RESULTS

Overview spectra for the $A^2\Delta$-$X^2\Pi$ electronic transition, as obtained using the pinhole discharge nozzle, are shown in the upper traces of Fig.1 for C_5H (Fig.1(a)) and C_5D (Fig.1(b)). The C_5D spectrum is ∼35 cm^{-1} blue-shifted with respect to the C_5H spectrum. In each spectrum a stronger and a weaker band are clearly visible, despite of a partial spectral overlap with narrow features. To reduce the spectral congestion, a Doppler-free spectrum has been recorded for C_5H using the slit discharge nozzle. The resulting spectrum is shown in Fig.2(a) for a laser bandwidth of ∼0.07 cm^{-1}. Figure 2(b) shows the spectrum in the same frequency range but recorded for a much lower backing pressure of ∼0.2 MPa. The latter conditions do not favor C_5H formation and only spectral features of small hydrocarbon compounds, such as C_2, C_3, CH, *etc.* are found. It is obvious that without these overlapping transitions the broad profiles in Fig.2(a) are identical to the mass-selective spectra recorded in the REMPI-TOF work (see the inset Fig.1 of Ref.[9]).

The $A^2\Delta$-$X^2\Pi$ transition of C_5H consists of two relatively broad and unresolved components. The stronger feature is at ∼18785.5(2) cm^{-1} and the weaker at ∼18760.4(2) cm^{-1}. For a regular $X^2\Pi$ ground state with an A'' value of ∼23.68 cm^{-1} [7], and for the low rovibronic temperatures in the plasma jet expansion,

DOI:10.1088/1674-0068/25/02/129-134

TABLE I $^2\Delta$ upper state parameters for C_5H and C_5D (all values are in cm^{-1}).

	$A^2\Delta$-$X^2\Pi$	CRD				REMPI-TOF [9]	
		ν	$(\nu_D-\nu_H)^a$	B'/B''^b	A'	ν	$(\nu_D-\nu_H)^a$
C_5H	0_0^0	18772.1(3)		1.06±0.04	−0.7±0.3		
	$A^2\Delta_{3/2}$-$X^2\Pi_{1/2}$	18785.5				18791	
	$A^2\Delta_{5/2}$-$X^2\Pi_{3/2}$	18760.4					
C_5D	0_0^0	18806.5	34.4	1.06[c]	(−1,0)[d]		
	$A^2\Delta_{3/2}$-$X^2\Pi_{1/2}$	18820.6	35.1			18824	33
	$A^2\Delta_{5/2}$-$X^2\Pi_{3/2}$	18794.7	34.4				

[a] The isotopic shift of the band position of C_5D with respect to C_5H.
[b] The B'/B'' ratio is dimensionless, where B'' are fixed to the values available in Refs. [7, 8].
[c] Fixed.
[d] The accurate value can not be determined.

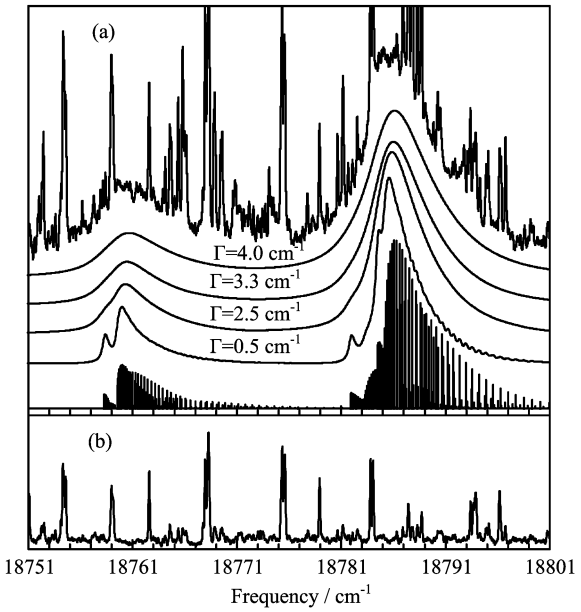

FIG. 2 (a) Recorded spectrum of the $A^2\Delta$-$X^2\Pi$ origin bands in C_5H using the slit discharge nozzle (upper trace) with a backing pressure of ∼1 MPa. Simulated spectra for different Lorentzian line width values (Γ=0.5, 2.5, 3.3, and 4.0 cm^{-1}) are shown in the middle trace. The stick diagram for a $A^2\Delta$-$X^2\Pi$ transition is shown in the lower trace. (b) Recorded absorption spectrum of the $A^2\Delta$-$X^2\Pi$ origin bands in C_5H using the slit discharge nozzle with a backing pressure of ∼0.2 MPa. In both panels a laser bandwidth of 0.07 cm^{-1} is used.

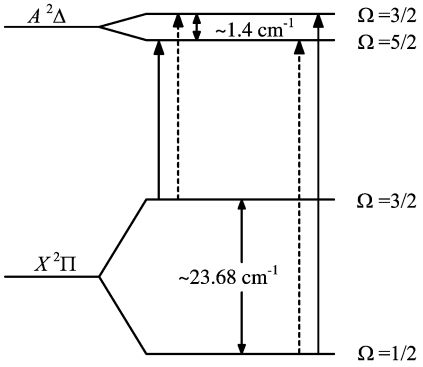

FIG. 3 Schematic energy level diagram for the $X^2\Pi$ and $A^2\Delta$ electronic states of C_5H. Solid-line arrows indicate the observed $A^2\Delta_{3/2}$-$X^2\Pi_{1/2}$ and $A^2\Delta_{5/2}$-$X^2\Pi_{3/2}$ bands. The dashed arrows represent the intrinsically weak (and not observed) $A^2\Delta_{5/2}$-$X^2\Pi_{1/2}$ and $A^2\Delta_{3/2}$-$X^2\Pi_{3/2}$ transitions.

the lower $^2\Pi_{1/2}$ component is expected to be more populated than the higher $^2\Pi_{3/2}$ component. Actually, the relative intensity ratio is a measure for the cooling efficiency in the expansion. Consequently, the bands at 18785.5 and 18760.4 cm^{-1} can be assigned as the $A^2\Delta_{3/2}$-$X^2\Pi_{1/2}$ and $A^2\Delta_{5/2}$-$X^2\Pi_{3/2}$ components, respectively.

The effective splitting of the maxima (Δ_{SO}) of the two bands amounts to ∼25.1 cm^{-1}, and is just a little larger than the A''-value. It reflects the net difference in spin-orbit splitting in ground and electronically excited state; $\Delta_{SO}=|A'\Lambda'-A''\Lambda''|$, where Λ=0, 1, and 2 depend on the Σ, Π, and Δ character of the electronic state, respectively, *i.e.* for a $^2\Delta$-$^2\Pi$ transition here, $\Delta_{SO}=|2A'-A''|$. The transition starting from the $^2\Pi_{1/2}$ component is located at higher energy than the one starting from the $^2\Pi_{3/2}$ component. As the ground state is regular this means that the excited state must be inverted with the $\Delta_{5/2}$ level below the $\Delta_{3/2}$ level.

In Fig.3 schematic energy level diagram is shown, summarizing these findings and explicitly including the spin-orbit splitting of both the $^2\Pi$ ground and $^2\Delta$ electronically excited state. This yields an estimated value of $A'\approx-0.7$ cm^{-1}. This A' value has not been derived in Ref.[9] where the assignment of the band system to a $A^2\Delta$ was based on the outcome of *ab initio* predictions. The present non-zero spin-orbit value in the upper state provides additional experimental evidence for the correct assignment of the observed spectrum to an excited $^2\Delta$ state, as the $^2\Sigma^{+/-}$ states should not exhibit any

DOI:10.1088/1674-0068/25/02/129-134

spin-orbit splitting.

It should be noted that for such a weak spin-orbit coupling, the $^2\Delta$ excited state of C_5H is not a typical electronic state characterized by Hund's case (a), because of spin-uncoupling [15]. In this specific case, rovibronic transitions corresponding to $A^2\Delta_{5/2}$-$X^2\Pi_{1/2}$ and $A^2\Delta_{3/2}$-$X^2\Pi_{3/2}$ are also allowed, but they will be much weaker with respect to the $A^2\Delta_{3/2}$-$X^2\Pi_{1/2}$ and $A^2\Delta_{5/2}$-$X^2\Pi_{3/2}$ bands, and are not resolved here. These weak transitions have been taken into account in the simulated stick diagrams shown in Fig.1 and Fig.2.

The extracted values for the individual band positions are listed in Table I. The resulting origin band value is given as well. In Ref.[9] only the maximum values for the stronger spin-orbit components are listed; 18791 cm^{-1} for C_5H and 18824 cm^{-1} for C_5D. These values are found to deviate from the values reported here: 18785.5 and 18820.6 cm^{-1}, respectively. It is unclear where this discrepancy comes. The present work relies on an absolute laser frequency calibration by simultaneously recording I_2 reference spectra (see Fig.1 where the synthetic I_2 spectrum is shown as well) that are accurate within 0.02 cm^{-1}. A likely explanation is that the wavelengths and wavenumbers in Ref.[9] are given in air and have not been corrected for vacuum.

The observed bands are unresolved, even though the rotational constant B'' of C_5H is $\sim$ 0.08 cm^{-1}, and a $\sim 2B$ rotational progression therefore should be easily resolvable within the experimental settings. This is illustrated by the artificial spectrum, shown as stick diagrams in Fig.1 and Fig.2, and simulated for a temperature of $\sim$30 K using PGopher [16]. The logical explanation for this observation is that the broadening is intrinsic and that the transitions to the $A^2\Delta$ upper state must be lifetime broadened. This will be discussed later. Nevertheless, it is still possible to obtain information on the rotational constants for the excited state.

Empirical rotational contour fits of the observed spectra are performed using a standard Hamiltonian for a $^2\Delta$-$^2\Pi$ transition. The ground state constants (B'', A'') are fixed to the available accurate values [7], while the excited state parameters (B', A', and the band origin ν_{00}), as well as the Lorentzian linewidth (Γ), can be varied to reproduce the experimental spectra. The best spectrally fitted contour for the C_5H band shown in Fig.2 is found for $A' \approx -0.7$ cm^{-1}, and a $B'/B'' \approx 1.06$ and (a Lorentzian linewidth) $\Gamma \approx 3.3$ cm^{-1}. This B'/B'' ratio is unexpected. For the other linear hydrocarbon chains whose electronic spectra can be rotationally resolved, it was found that the overall chain length slightly increases upon electronic excitation, resulting in a typical B'/B'' ratio smaller than 1 [11−13, 17−19]. The derived $B'/B''>1$ value means that the length of C_5H decreases upon electronic excitation. To confirm this finding, the stronger C_5H spin-orbit component at $\sim$18785.5 cm^{-1} has been recorded using the slit discharge nozzle at the best possible laser bandwidth of $\sim$0.035 cm^{-1}.

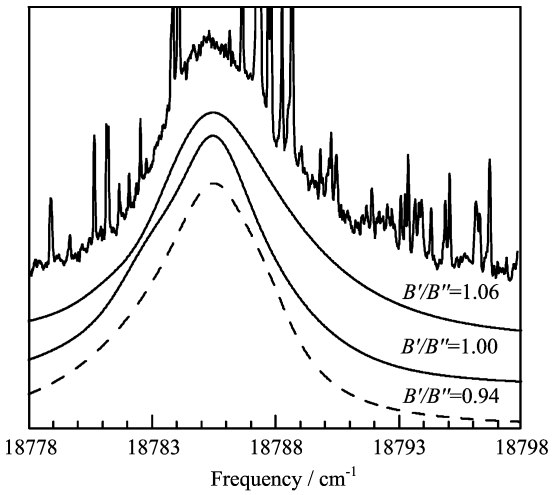

FIG. 4 A 0.035 cm^{-1} recording of the $A^2\Delta_{5/2}$-$X^2\Pi_{3/2}$ spin-orbit component of C_5H (upper trace). The lower traces show simulated spectra for three different B'/B'' ratios.

The resulting spectrum is shown in the upper trace of Fig.4. As the band is featureless, special care has been taken to exclude the risk that the band profile is overfit. Instead the reliability of the spectral fitting is verified by varying the B'/B'' ratio from 0.9 to 1.1. This shifts the resulting value for the band origin (T_{00}) from 18771.8 cm^{-1} to 18772.4 cm^{-1} but it does not influence the derived $A' = -0.7(3)$ cm^{-1} value. Simulated band contours are shown in the lower traces of Fig.4 for B'/B''=1.06, 1.00, and 0.94. The observed band profile is indeed best fitted for a $B'/B'' \approx 1.06 \pm 0.04$ ratio. This confirms that in this specific case the effective length of the chain seems to shrink and a possible (but not conclusive) explanation could be that the potential surface of the $A^2\Delta_{3/2}$ state of l-C_5H chain has an energy minimum in a non-linear geometry due to Renner-Teller effect, as found for l-C_3H [20].

As stated above, the unresolved bands are indicative for an intrinsic lifetime broadening. In the spectral simulation, a Gaussian linewidth of $\sim$0.12 cm^{-1} is used. To reproduce the experimental spectrum shown in Fig.2, the Lorentzian linewidth has to be determined. Simulated band contours for values of Γ=0.5, 2.5, 3.3, and 4 cm^{-1} are shown in Fig.2. Even though this is only an approximate way of determining the Lorentzian width, the observed profile is clearly best simulated for a value of $\Gamma = 3.3 \pm 0.5$ cm^{-1} (for $T_{rot} \approx 26$ K). This value for the Lorentzian line broadening parameter corresponds to a lifetime of (1.6±0.3) ps for the upper $^2\Delta$ state of C_5H.

Many of the conclusions derived above for C_5H also apply to C_5D. The rotational and spin-orbit coupling constants for the $X^2\Pi$ ground states of l-C_5D have been reported in Ref.[8]. The band positions of the $A^2\Delta_{3/2}$-$X^2\Pi_{1/2}$ and $A^2\Delta_{5/2}$-$X^2\Pi_{3/2}$ transitions are found at $\sim$18820.6 and $\sim$18794.7 cm^{-1}, respectively, and the re-

DOI:10.1088/1674-0068/25/02/129-134

sulting effective spin-orbit splitting (Δ_{SO}) amounts to $\sim$25.9 cm^{-1}. An empirical contour fit is applied to the observed C_5D spectrum, fixing the available ground state parameters in Ref.[8] and using the same values for B'/B'' ratio and Lorentzian width Γ that are derived for C_5H above. From this analysis, the value for the spin-orbit coupling constant A' is found to be between 0 and -1.0 cm^{-1}. The substantial overlap of narrow features with the weak $A^2\Delta_{5/2}$-$X^2\Pi_{3/2}$ component does not allow a more accurate determination of this value. All relevant values are summarized in Table I.

IV. DISCUSSION

The magnitude of the deduced spin-orbit coupling constants A' in the $A^2\Delta$ state of C_5H is much smaller than that in its $X^2\Pi$ ground state. Similar behavior has also been observed for CH ($A''\approx$28.05 cm^{-1}, $A'\approx-1.0$ cm^{-1}) [21−23] and C_3H ($A''\approx$14.2 cm^{-1}, $A'\approx$0) [20, 24] radicals. It is noted that the three hydrocarbons $C_{2n+1}H$ (n=0−2) have similar electronic configuration in their $X^2\Pi$ ($\cdots\sigma^2\pi^1$) and $A^2\Delta$ ($\cdots\sigma^1\pi^2$) states, where the $A^2\Delta$ state of C_3H splits into two A^2A' and B^2A'' states because of very strong Renner-Teller effect [20, 25−28]. The comparable spin-orbit coupling constant between CH and C_5H indicates that the spin-orbit coupling in $X^2\Pi$ and $A^2\Delta$ states of C_5H may originate from the one-electron spin-orbit coupling in atomic $2p_\pi$ orbitals of C(^{3}P, $2s^22p^2$) and C($^3D_0$, $2s^2p^3$), respectively.

Further, previous work shows that, because of very strong Renner-Teller effect [20, 24−28], the effective spin-orbit coupling constants of C_3H have become much smaller than those of CH, particularly in the $A^2\Delta$ state of C_3H the spin-orbit coupling have been completely quenched. Here, the result that both spin-orbit coupling constants in $X^2\Pi$ and $A^2\Delta$ states of C_5H are slightly smaller than those for CH, respectively, may hint at significant Renner-Teller effects in both states of C_5H, but the Renner-Teller effect for C_5H should be weaker than that for l-C_3H.

The short lifetime of the excited state of C_5H, $\sim$1.6 ps, must be due to a fast radiationless process, most likely a strong intramolecular interaction, as all possible dissociation or isomerization products of l-C_5H lie energetically higher than the $A^2\Delta$ state [5]. It is expected that l-C_5H in its $X^2\Pi$ ground state also exhibits a substantial Renner-Teller effect. Theoretical calculations have predicted a large splitting ($\sim$100 cm^{-1}) for the lowest bending vibrational mode ν_9 owing to strong Renner-Teller interaction in the ground state of l-C_5H [5]. Highly excited vibronic levels with Δ symmetry in the $X^2\Pi$ ground state therefore are expected to be close to the $A^2\Delta$ state and eventually to strongly interact with the $A^2\Delta$ electronic state via vibronic couplings. Such couplings offer a possible relaxation channel responsible for the observed short lifetimes in the excited states of the l-$C_{2n+1}H$ homologous series. A more detailed picture of the exact nature of the internal conversion process is not available at this stage.

V. CONCLUSION

An improved interpretation of recalibrated $A^2\Delta$-$X^2\Pi$ electronic origin band transitions of l-C_5H and l-C_5D is presented. It has been possible to derive accurate band positions and to determine the spin-orbit coupling constants in the upper states for both isotopologues. The broadening of the spectra is interpreted in terms of a short lifetime of (1.6±0.3) ps for the $A^2\Delta$ state which is likely associated with strong vibronic couplings.

VI. ACKNOWLEDGMENTS

This work was supported by the Netherlands Foundation for Fundamental Research of Matter. The work has been performed within the context of the Dutch Astrochemistry Network NWO program. Harold Linnartz thanks Stichting Physica. Mohammad Ali Haddad thanks the Iran Ministry of Science, Research and Technology for financial supports. Samples of C_2D_2 were generously made available by Prof. S. Schlemmer from University of Cologne.

[1] M. B. Bell, P. A. Feldman, J. K. G. Watson, M. C. McCarthy, M. J. Travers, C. A. Gottlieb, and P. Thaddeus, Astrophys. J. **518**, 740 (1999).
[2] M. Guelin, J. Cernicharo, M. J. Travers, M. C. McCarthy, C. A. Gottlieb, P. Thaddeus, M. Ohishi, and S. Saito, Astron. Astrophys. **317**, L1 (1997).
[3] J. Cernicharo, M. Guelin, and C. M. Walmsley, Astron. Astrophys. **172**, L5 (1987).
[4] J. Cernicharo, C. Kahane, J. Gomez-Gonzalez, and M. Guelin, Astron. Astrophys. **164**, L1 (1986).
[5] T. D. Crawford, J. F. Stanton, J. C. Saeh, and H. F. Schaefer, J. Am. Chem. Soc. **121**, 1902 (1999).
[6] F. Pauzat, Y. Ellinger, and A. D. McLean, Astrophys. J. **369**, L13 (1991).
[7] C. A. Gottlieb, E. W. Gottlieb, and P. Thaddeus, Astron. Astrophys. **164**, L5 (1986).
[8] T. Hirota, H. Ozawa, Y. Sekimoto, and S. Yamamoto, J. Mol. Spectrosc. **174**, 196 (1995).
[9] H. Ding, T. Pino, F. Guthe, and J. P. Maier, J. Chem. Phys. **117**, 8362 (2002).
[10] J. Haubrich, M. Muhlhauser, and S. D. Peyerimhoff, J. Phys. Chem. A **106**, 8201 (2002).
[11] D. Zhao, M. A. Haddad, H. Linnartz, and W. Ubachs, J. Chem. Phys. **135**, 044307 (2011).
[12] N. Wehres, D. Zhao, H. Linnartz, and W. Ubachs, Chem. Phys. Lett. **497**, 30 (2010).
[13] D. Zhao, N. Wehres, H. Linnartz, and W. Ubachs, Chem. Phys. Lett. **501**, 232 (2011).

DOI:10.1088/1674-0068/25/02/129-134

[14] T. Motylewski and H. Linnartz, Rev. Sci. Instrum. **70**, 1305 (1999).
[15] G. Herzberg, *Molecular Spectra and Molecular Structure I. Spectra of Diatomic Molecules*, 2nd Edn., New York: D. Van Nostrand, 231 (1950).
[16] PGOPHER, *A Program for Simulating Rotational Structure*, C. M. Western, University of Bristol, Available from: http://pgopher.chm.bris.ac.uk.
[17] P. Birza, T. Motylewski, D. Khoroshev, A. Chirokolava, H. Linnartz, and J. P. Maier, Chem. Phys. **283**, 119 (2002).
[18] D. Pfluger, T. Motylewski, H. Linnartz, W. E. Sinclair, and J. P. Maier, Chem. Phys. Lett. **329**, 29 (2000).
[19] H. Linnartz, T. Motylewski, O. Vaizert, J. P. Maier, A. J. Apponi, M. C. McCarthy, C. A. Gottlieb, and P. Thaddeus, J. Mol. Spectrosc. **197**, 1 (1999).
[20] H. Ding, T. Pino, F. Guthe, and J. P. Maier, J. Chem. Phys. **115**, 6913 (2001).
[21] M. Zachwieja, J. Mol. Spectrosc. **170**, 285 (1995).
[22] Z. Bembenek, R. Kepa, A. Para, M. Rytel, M. Zachwieja, J. D. Janjić, and E. Marx, J. Mol. Spectrosc. **139**, 1 (1990).
[23] G. Herzberg, J. W. C. Johns, Astrophys. J. **158**, 399 (1969).
[24] P. Thaddeus, C. A. Gottlieb, A. Hjalmarson, L. E. B. Johansson, W. M. Irvine, P. Friberg, and R. A. Linke, Astrophys. J. **294**, L49 (1985).
[25] M. Peric, M. Mladenovic, K. Tomic, and C. M. Marian, J. Chem. Phys. **118**, 4444 (2003).
[26] F. J. Mazzotti, R. Raghunandan, A. M. Esmail, M. Tulej, and J. P. Maier, J. Chem. Phys. **134**, 164303 (2011).
[27] S. M. Sheehan, B. F. Parsons, J. Zhou, E. Garand, T. A. Yen, D. T. Moore and D. M. Neumark, J. Chem. Phys. **128**, 034301 (2008).
[28] R. K. Chaudhuri, S. Majumder, and K. F. Freed, J. Chem. Phys. **112**, 9301 (2000).

DOI:10.1088/1674-0068/25/02/129-134